

Formation processes of a reopened early Bronze Age inhumation grave in Austria: the soil thin section analyses

Article

Published Version

Creative Commons: Attribution 4.0 (CC-BY)

Open Access - In Press Corrected Proof

Aspöck, E. and Banerjea, R. Y. ORCID: <https://orcid.org/0000-0002-1786-357X> (2016) Formation processes of a reopened early Bronze Age inhumation grave in Austria: the soil thin section analyses. *Journal of Archaeological Science: Reports*, 10. pp. 791-809. ISSN 2352-409X doi: 10.1016/j.jasrep.2016.07.003 Available at <https://centaur.reading.ac.uk/66774/>

It is advisable to refer to the publisher's version if you intend to cite from the work. See [Guidance on citing](#).

To link to this article DOI: <http://dx.doi.org/10.1016/j.jasrep.2016.07.003>

Publisher: Elsevier

All outputs in CentAUR are protected by Intellectual Property Rights law, including copyright law. Copyright and IPR is retained by the creators or other copyright holders. Terms and conditions for use of this material are defined in the [End User Agreement](#).

www.reading.ac.uk/centaur

CentAUR

Central Archive at the University of Reading

Reading's research outputs online



Contents lists available at ScienceDirect

Journal of Archaeological Science: Reports

journal homepage: www.elsevier.com/locate/jasrep

Formation processes of a reopened early Bronze Age inhumation grave in Austria: The soil thin section analyses

Edeltraud Aspöck^{a,*}, Rowena Yvonne Banerjea^b

^a OREA Institute for Oriental and European Archaeology, Austrian Academy of Sciences, Hollandstrasse 11-13, 1020 Vienna, Austria

^b Quaternary Scientific, School of Archaeology, Geography, and Environmental Science, University of Reading, Whiteknights, RG6 6AB, United Kingdom

ARTICLE INFO

Article history:

Received 18 October 2015

Received in revised form 23 June 2016

Accepted 3 July 2016

Available online xxxx

Keywords:

Soil micromorphology

Burial taphonomy

Grave reopening

Grave formation processes

Bronze Age

Wieselburg Gáta culture

ABSTRACT

Early Bronze Age and early medieval inhumation graves in (central) Europe had often been re-opened a short time after burial and, in most cases, grave goods were removed. To improve the understanding of the archaeological evidence of these graves, one re-opened grave from a large early Bronze Age (Wieselburg/Gáta culture) cemetery in Weiden am See, eastern Austria, was excavated using a microstratigraphic protocol to maximize data collection for the reconstruction of the context formation process and, consequently, the interpretation of the re-opening process. In this article the results of the soil thin section analyses are presented and discussed.

© 2016 The Authors. Published by Elsevier Ltd. This is an open access article under the CC BY license (<http://creativecommons.org/licenses/by/4.0/>).

1. Introduction

To improve our understanding of formation processes of reopened graves and to create a reference for future analyses, a reopened inhumation grave at the early Bronze Age cemetery of Weiden am See, eastern Austria, was excavated and examined using a microstratigraphic approach. A combination of methods was applied to maximize the range of data to use to reconstruct formation processes at excavation (single-finds recording, wet-sieving of sediments) and post-excavation (micromorphology, geochemical and mineralogical characterization of sediments, radiocarbon dating, 3D visualization of archaeological features and integration with results of post-excavation analysis). However, this paper will focus on the micromorphology results, as this analysis provides the crucial microstratigraphic framework for interpreting the depositional sequence and formation processes within the grave, and is the basis for which the results of other proxies can be integrated.

The Wieselburg/Gáta Culture is an early Bronze Age Culture (2000–1600 BCE, Bronze Age A2) located in eastern Austria and west Hungary, south of the Danube, as well as parts of south-western Slovakia (Hicke, 1987; Krenn-Leeb, 2011; Leeb, 1987). Cemeteries contained up to a few

hundred graves where the dead were typically buried in individual graves in coffins or stone settings, accompanied by jewelry (copper alloy jewelry and necklaces with amber beads, animal teeth) and copper alloy objects (e.g. daggers) and pottery. The bodies were oriented southwest-northeast (women on their right and men on their left sides) with their lower limbs in flexed or hyperflexed position. It was common that the graves were reopened and copper alloy objects were removed. The position of the finds and skeleton attest to reopening that usually took place not long after burial; there is evidence that bodies were not fully decomposed when this reopening occurred and hollow spaces permitted movement within the graves (Neugebauer, 1988).

Generally, central European early Bronze Age and early medieval period inhumation cemeteries often contain large numbers of graves that were reopened soon after burial, usually with evidence for removal of grave goods (Aspöck, 2005, 2011, 2015; Aspöck and Klevnäs, 2011; Klevnäs, 2013; Kümmel, 2009; Neugebauer, 1991; Neugebauer-Maresch and Neugebauer, 1997; Rittershofer, 1987; Sprenger, 1999; van Haperen, 2010; Zintl, 2012). This phenomenon has traditionally been interpreted as ‘grave robbery’, i.e. looting of graves driven by purely materialistic motives. More recent research has questioned this interpretation by examining reopening practices from a broader perspective, leveling hypotheses and case studies drawn from social anthropological research (e.g. Aspöck, 2005: 226–235; Kümmel, 2009; van Haperen, 2010, 2013). In particular, the

* Corresponding author.

E-mail addresses: edeltraud.aspoeck@oeaw.ac.at (E. Aspöck), r.y.banerjea@reading.ac.uk (R.Y. Banerjea).

discussion on early medieval grave reopening has been lively and has resulted in differentiation of types of 'grave robbery' (Aspöck, 2011, 2015; Aspöck and Klevnäs, 2011; Aspöck et al., 2016; Klevnäs, 2007, 2013, 2015; van Haperen, 2010, 2013; Zintl, 2012).

However, analysis and interpretation of reopened graves often ends where the archaeological evidence is poorly understood. It is, for example, often difficult to distinguish between the results of natural processes of decomposition and of human intervention in a grave. Generally, decomposition processes play an important role in the interpretation of reopened graves because the state of the body and grave furniture upon reopening can potentially be inferred from the archaeological evidence, providing a timeframe for the reopening of the grave. Hence, understanding decomposition processes and, in a wider sense, the formation processes of the archaeological evidence of reopened inhumation graves is crucial for their interpretation. In a pilot study, one reopened grave in an Austrian Wieselburg Culture cemetery was excavated using a microstratigraphic method to maximize data for the reconstruction of specific, complex depositional and post-depositional processes within this grave (Table 1).

Micromorphology is well established as a tool for interpreting archaeological site formation processes. The technique has been widely applied to understand and interpret the use of settlement space (e.g. Banerjea et al., 2015a; Matthews, 1995; Shahack-Gross et al., 2005; Shillito and Ryan, 2013) and the reworking of archaeological stratigraphy by post-depositional processes (e.g. Canti, 2003; Devos et al., 2009; French, 2003: 123, 156; Gé et al., 1993; Macphail, 1994; Macphail et al., 2003; Weiner, 2010).

Table 1
Research questions with linked micromorphology samples.

1. What was the original appearance of the grave (burial of individual 2) before the reopening?
 - Sample 450: Are there remains of the top coffin board in this sample? What type of deposit is SE6, which was the top layer inside the coffin - is it the remains of a wooden board? What are the differences between the sediments above and inside the coffin?
 - Sample 454: What is the nature of the grey-lilac layer (SE12; Munsell® color, 2000 2.5Y 7/1) which outlines the vertical shape of the coffin?
 - Sample 669: What was the nature of sediments underneath the space of the coffin where not affected by the reopening?
2. When and how did the reopening of the grave take place?
 - Samples 310, 311 (lower area of profile): was this the refill of the intervention pit or original grave fill?
 - Sample 454: What are the differences (deposit and formation types) between the original grave fill outside of the coffin and the refill of the intervention pit?
3. What kind of grave manipulations took place upon reopening?
 - Is there evidence for micro remains from grave goods that have been removed in any of the samples?
4. When and how did the refilling after the reopening take place? Was the grave refilled immediately – by human activity, or did it refill slowly and naturally, or were there more episodes of refilling?
 - Sample 364: Is this the refill of the intervention pit or erosion after intervention? How is this sediment different to the grave fill?
 - Sample 366: Original grave fill or intervention pit refill (compare to sample 364)?
 - Samples 451, 470, 471, 592: How did the refill of the intervention pit take place – quick or slow? Is there evidence for weathering or fine sedimentation in this area? Are there micro-remains from (human) bone?
5. How did natural formation processes affect the final archaeological evidence of a reopened grave?
 - Sample 591: What is the nature of the sandy sediments in the coffin? How have they been deposited?
 - Sample 642: What is the nature of the sediments underneath the left tibia and fibula – how did they form?
6. What was the original appearance of the top burial (individual 1)?
 - Samples 250, 251: was the surface of SE2 a pit that was left from the reopening or was a separate pit cut for SE1 and burial 1, and if yes, was it left open or refilled immediately?
 - Samples 189, 226: Is it possible to find surfaces/interfaces around the body of individual 1? Was the body put directly on the soil and was there a hollow space around the body (e.g. wooden structure)?

Micromorphological examination of graves is an understudied area of research (Kutterer et al., 2014a, 2014b: 181) without the wealth of published comparative case studies or experimental material that is available for the study of the use of settlement space. This problem should be able to be addressed with the conclusion of the InterArChive project (Usai et al., 2014), which will provide interpretative frameworks for more robust micromorphological examinations of grave taphonomy. Micromorphology provides significant potential for understanding the depositional formation processes and post-depositional alterations (Macphail et al., 2013) relating to burial taphonomy, particularly for disturbed graves (Huckleberry et al., 2003) and sedimentation rates within burials (Sandgathe et al., 2011).

Within graves there can be considerable variation in chemistry and micromorphology on both intra- and inter-site level, linked to environmental contrasts and taphonomic variation. Post-burial changes are highly complex, and there can be evidence for mobilisation/depletion, transportation and re-deposition of soil/sediment displaying preferential spatial patterns in relation to the different parts of skeletons and graves (Usai et al., 2014). In particular, the area below the cranium has been identified as an area for processes relating to calcite mobilisation and sedimentation (Kutterer et al., 2014a, 2014b: 181).

This paper aims to examine how micromorphology can contribute to reconstruct the formation process and to answer the following research questions that are typically asked for reopened graves with specific reference to key questions pertaining to the buried human remains (Table 1):

1. What was the original appearance of the grave before the reopening?
2. When and how did the reopening of the grave take place?
3. What kind of grave manipulations took place upon reopening?
4. When and how did the refilling of the grave take place? Was the grave refilled immediately – by human activity, or did it refill slowly and naturally, or were there more episodes of refilling?
5. How did natural formation processes affect the final archaeological evidence of the reopened grave?

2. Material and methods

2.1. Site and excavation

Weiden am See, Austria, is a multi-period site (Fig. 1) located 1 km off the contemporary shores of Lake Neusiedl, a 35 km long and <2 m deep endorheic lake in the Austrian-Hungarian border lands (Hicke, 1987: 14). Since 2012, rescue excavations have recovered over 200 early Bronze Age of the Wieselburg Culture graves, around half of them reopened (Fig. 2, Franz et al., 2014).

In 2013 one grave (object 229, MNR 32026.13.03, Gst 1023/439-444) was excavated with close attention to the evidence for reopening (Video 1: excavation process). As part of the rescue excavations, about 1 m of topsoil had already been removed with a digger, and the outline of a large grave pit with set blocks of stone and some human bones (a humerus and a femur) were visible at the beginning of the excavation. The excavation identified stratigraphic units and, where relevant, additional surfaces within these units. The grave was half-sectioned after excavation of the top individual to determine the depth of the grave and to ascertain if there would be more individuals buried underneath.

Documentation included drawing plans, three-dimensional single-finds recording (all finds larger than 1 cm), and the documentation of all features (outlines, surfaces, boundaries) using a Leica Tachymeter TCR 407 controlled by a field computer (Dibble and McPherron, 1991; Händel, 2010). The evidence was photographed from a ladder/elevated position so that the resulting photographs were as close as possible to directly overhead. These vertical images covered the complete feature. Additionally, many oblique shots were taken to capture details, which later allowed the use of the complete image collection in an image-based modelling workflow (Video 1: excavation process). All excavated



Video 1. Movie of 3D model Weiden am See 2013/object 229: Photographs of each excavated layer were used to create separate georeferenced 3D models using the image-based modelling software package Agisoft Photoscan Professional. The video depicts 3D models of layers and their removal according to the excavation process and the position of the samples. The missing data (of layer S02) is marked with blue color.

sediments were wet-sieved (sieve mesh size 2 mm), except for parts of SE3 (the original grave fill), which for time reasons was not sieved, but searched through twice by hand, when it became apparent that the grave was much deeper than anticipated. The excavation method was very time-consuming and excavation of the grave took over two months, with 2–3 people working at a time on the excavation and wet-sieving of the sediments.

2.2. Sampling strategy

Collection of soil micromorphology samples was guided by the above research questions for reopened graves (Table 1). Samples were taken from the different types of fills and at important locations and interfaces (Fig. 3, Video 1 and Supplement 1), such as the disturbed area of the coffin at the bottom of the grave. The sampling of the undisturbed upper inhumation was influenced by a strategy developed as part of the InterArChive project (Usai et al., 2014) and samples from above, below, and at the sides of the skeleton were collected, as well as geological reference samples from a profile further away from the skeleton (Fig. 4). As part of this project only some samples for comparison of the two buried individuals were selected for analysis. Kubiena tins in three different sizes were used to collect the samples and very small

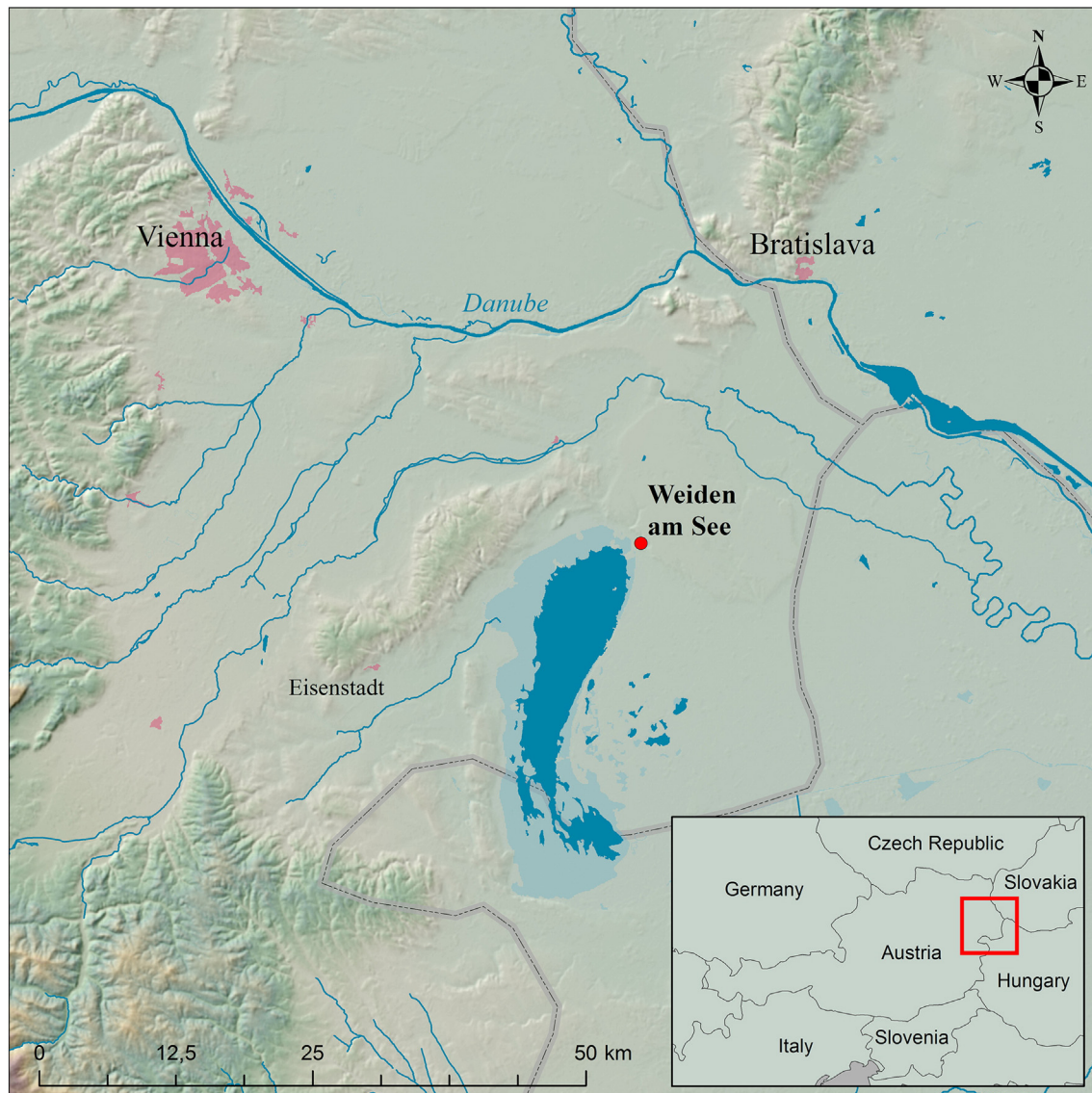


Fig. 1. Weiden am See at Lake Neusiedl, Austria. Map based on NASA SRTM3.



Fig. 2. Location of the grave 'Weiden am See 1023/object 229' (MNR 32026.13.03, Gst 1023/439–444) in the context of the early Bronze Age cemetery Weiden am See with the graves marked in green. (For interpretation of the references to color in this figure legend, the reader is referred to the web version of this article.)

boxes proved useful in the area of comingled human remains to avoid damaging of bone. Except for the geology samples and three samples from the profile in the grave, the tins were pushed into the soil from above and then the soil around it removed. Before removal of the sample, the four top corners of the box were recorded with the tachymeter. Photos were taken before and after sampling and specific research questions for each of the samples were recorded. Loose soil samples were collected from the corresponding field units within the undisturbed micromorphology samples.

At excavation, 53 undisturbed micromorphology samples, including 7 reference samples of the six geological layers (Fig. 4) at the site were collected. 17 archaeological and 6 geological samples were selected for processing and analysis to answer research questions that could not be answered at excavation or that came up as part of the post-excavation process.

2.3. Laboratory methods: micromorphology

Micromorphology samples were prepared in the Microanalysis Unit, University of Reading. The procedure followed is the standard protocol for thin section preparation (Murphy, 1986). Samples were oven-dried at 40 °C, and then impregnated with epoxy resin while under vacuum. Slides were prepared to the standard geological thickness of 30 µm.

Micromorphological investigation was carried out using a Leica DMLP polarising microscope at magnifications of $\times 40$ – $\times 400$ under Plane Polarised Light (PPL), Crossed Polarised Light (XPL), and where appropriate Oblique Incident Light (OIL). Thin-section description was conducted using the identification and quantification criteria set out by Bullock et al. (1985) and Stoops (2003), with reference to Courty et al. (1989). Photomicrographs were taken using a Leica camera attached to the Leica DMLP microscope.

3. Results

3.1. Observations at excavation (Table 2; Figs. 5 and 6; Video 1 and Supplement 1)

The movie of the 3D model of the grave (Video 1) shows the excavation process and the position of the micromorphology samples in the grave. The stratigraphic sequence observed at excavation is linked to the micromorphology samples (Figs. 5 and 6, Table 2). The top layer of organic silty loam (SE1) contained a setting of large stone blocks surrounding a body (Individual 1), buried prone (i.e. face-down) with the lower limbs flexed and descending inferiorly (Fig. 3). No surfaces/structures were visible to outline the space into which the body had been placed, other than the stones (66, 67, 68) and holes left from stones (5, 6) (removed by the excavator, on both sides of the body)

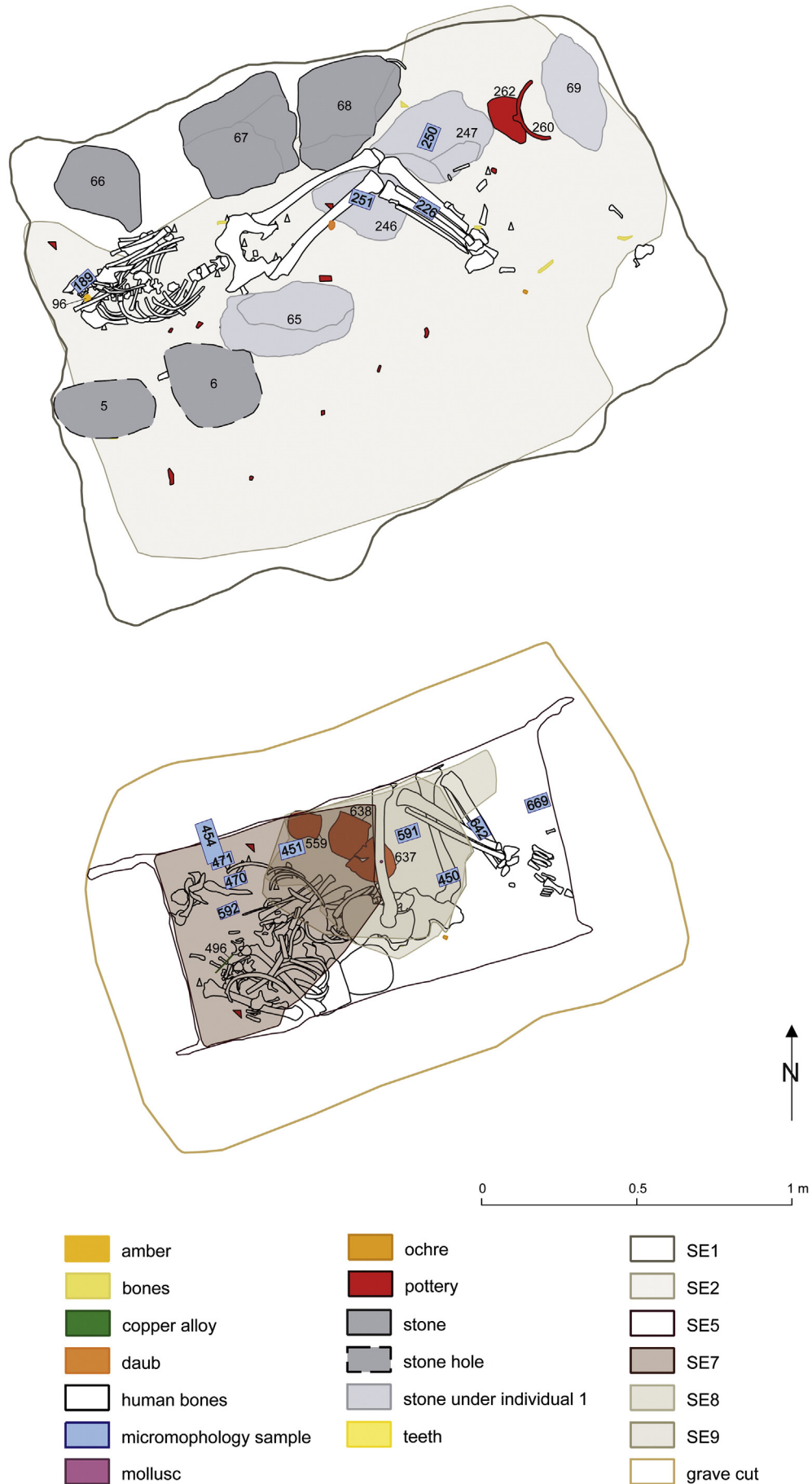


Fig. 3. 'Weiden am See 2013/object 229' top and bottom individual with location of the micromorphology samples.

surrounding the body, and stones (65, 246, 247) underneath the body. Samples were taken from underneath the body of individual 1 to see if a surface could be identified and to compare pedogenesis and chemical alterations with samples from underneath individual 2 inside the coffin: 189 (SE1 below a fragment of the mandible), 226 (SE1 below the tibiae and fibulae – analogue sample 642 below tibiae and fibulae of individual 2).

Underneath, the surface of SE2 formed an irregular pit and samples 250 and 251 were taken from the top surface of SE2 (Supplement 1) to establish if this was the surface of a pit that has been dug into the existing grave pit. SE2 was a heterogeneous and, in parts, a very organic fill, particularly in the western half of the grave pit, where it narrowed down into a funnel-like structure, remnants of the reopening pit (Supplement 1).

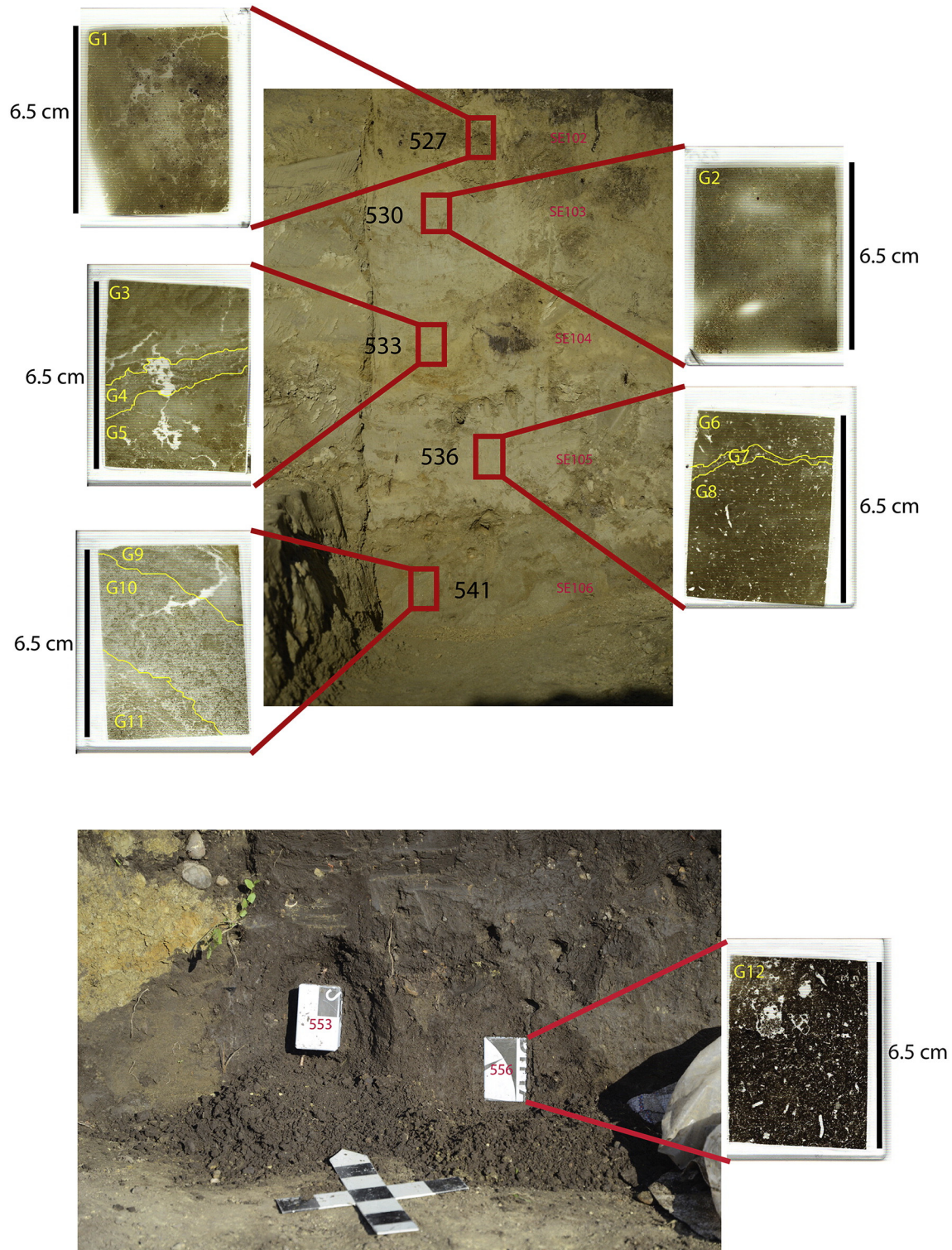


Fig. 4. Location photographs for geological samples and their associated thin-sections.

The 'funnel-like' structure identified at excavation was too small to represent the reopening pit and until the level of the coffin was reached, it remained uncertain whether this grave had actually been reopened.

Hence, five samples have been analyzed post-excavation to, among other things, define the boundaries of the reopening pit (SE2/SE3 interface) and the area of undisturbed grave fill SE3, a heterogeneous fill

Table 2

Summary stratigraphy table: stratigraphic units observed at excavation, their associated micromorphology samples and their interpretation at excavation.

	Stratigraphic unit	Associated MM samples	Description of sediment	Description of context	Interpretation
Top fill with individual 1	SE1	189, 226, (below individual 1)	Organic, homogeneous loamy silt.	SE1 with individual 1 buried in prone position between large blocks of stone and two halves of a vessel at west end of grave.	Large blocks of stones and body individual 1 deposited in very quick succession – no interface visible.
Pit	Interface SE1/SE2	250, 251		Irregular pit.	Pit dug for deposition of stones, pottery and body individual 1.
Refilled reopening pit	SE2	250, 251	Dark silty loam, very inhomogeneous. Same color as SE1, but with 10–40% large yellow patches, concentrations of ochre (FeO ₂) and pockets of gravel. Lighter in the eastern half of the pit and more organic towards the center and in the west.	SE2 stretched over most of the grave pit and was about 30–40 cm deep (east), while in the western half SE2 was going deeper forming a 'funnel'. Around the funnel many small pieces of ceramics and daub were found on the bottom of SE2.	SEs 2, 3A and 7 are the organic refill of the intervention pit. The top surface stretched over most of the grave pit (SE2) then continued inside a funnel (SE3A) and as a dark patch within SE3. At the bottom of the grave - inside the coffin this dark fill (SE7) seems to have preserved the original height of the coffin, while the eastern part of the coffin collapsed when the wood was decayed.
	SE3A	364	SE3A was dark silty loam with 5% large yellow patches. SE3 in the southwest corner fatty and organic, towards the bottom more light brown.	Inside the funnel SE3A went deeper, like a 'dark pocket' in SE3 below.	
	SE7	454 451 470, 592, 471	Dark and 5% lighter silty loam.	The very dark fill reached into the western part of the coffin (SE7) and the coffin was higher in this area.	
Reopening pit	Interface SE2,SE3A/SE3	366		Even in the eastern part of the grave, then forms slop and funnel in the west. Boundary more clear in east, unclear in other areas.	The funnel is what remained from the pit dug to reopen the grave.
Original grave fill	SE3	366 310 311 419	Heterogeneous fill consisting of light and dark loamy and silty patches. Silty patches increase with depth.	About 1.2 m deep, very heterogeneous layer nearly devoid of finds. More compact than SE2. Very dark and lighter pockets of sediments are alternating.	Grave fill, apparently material from different heaps of sediments was alternatingly deposited in the grave.
	SE5	450		On top of the coffin sandy and loamy yellowish sediments, with a patch of darker sediment next to the stone.	Grave fill above the coffin.
	SE15	454		Around the coffin, two types of yellowish sediments, no dark patches visible.	Grave fill around the coffin.
Coffin with individual 2	SE6	450	Very dark, about 1 cm thick layer, consistence soft (dry). The top was partly covered by a white/white-lilac substance (Munsell® color, 2000 2.5Y 7/1).	Very dark organic layer that covered most of the eastern half of the inner coffin area.	This may be the organic remains of a wooden board that covered the coffin.
	SE8	591 Sediment inside pot 638 and 637	Very sandy layer with a homogeneous brownish color.	Very distinct layer, the top layer of a heap of sandy material in the coffin area between the femora and trunk area.	Sediment that accumulated inside the coffin after burial when wood decayed through soil pressure or changing water levels.
	SE9	591, 450, 642 Sediment inside pot 638 and 637	Homogenous layer of brown sand mixed with darker (organic?) material, hardly any inclusions.	Bottom layer of the heap of sandy material inside coffin.	Did SE9 form because organic material accumulated in the bottom of the coffin E.g. rising and falling ground water levels washed soil particles from SE7 into SE8?
	Group 4			Skeleton individual 2 disturbed but undamaged in area of upper body (SE7/SE7A). Parts of a copper alloy pin with intermingled bone and 3 pots next to the body.	Body in flexed position, on left side, with pots and copper alloy jewelry, in coffin. When grave was reopened, joints still partly connected and coffin was intact.
	Coffin: SE11 –SE14, SE16	454 470, 471, 592, 642, 669	White/greyish/lilac powdery material (Munsell® color, 2000 2.5Y 7/1).	Material outlines a rectangular context, bottom (SE11), sides (SE12) strongly leaning inwards and vertical features (SE13) protruding 5–15 cm at the corners. Micro-contexts SE14 (light silty sediment) between handle and side of coffin and SE16 (triangular, silty in corner of SE11–13).	A coffin with handles, white-lilac material along the sides and bottom is typical for that period.
Grave pit	Interface Object 229	470, 592, 471,642, 669		Large rectangular pit narrowing down at the bottom. Rounded corners top surface.	Grave pit with evidence for grave markers (posts).
Geology	SE106	470, 592, 471,642, 669	Fine sand.	Sandy layer (gley) below the coffin of the grave.	Geology below the grave.

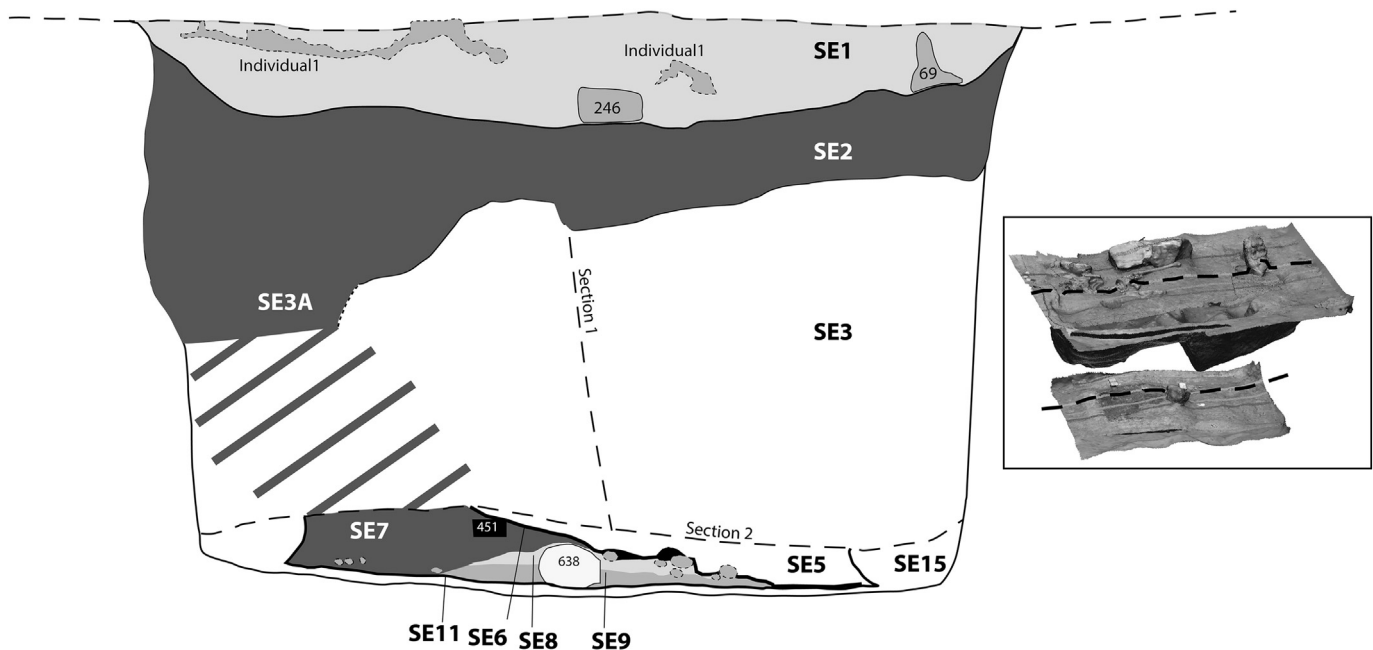


Fig. 6. Section drawing: Schematic section 'Weiden am See 2013/object 229' based on section through the 3D model.

Leeb, 2011). Just above and inside the coffin, the boundaries of the dark layer of refill of the reopening pit became very clear (SE7). Samples 454 and 450 (Fig. 3, Supplement 1) were taken to be able to characterise the refilling process (e.g. slow/natural or quick refill, and the number of refilling episodes). In this area of disturbance, the upper part of the body (individual 2) was disturbed, while outside this area, the lower limbs were undisturbed, showing that the individual had been placed with the lower limbs flexed on the left side. In the undisturbed area, a layer of very dark thin organic material covered the interior of the coffin (SE6) with again some greyish-white material on the top, like the outline of the coffin). Below SE6, a deposit of very sandy sediment (SE08) was found in the area between the femora and torso, with a more organic sandy layer underneath (SE09; samples 591, 450; samples 470, 592, Figs. 3 and 6, Supplement 1). Samples of the sandy layer were taken to investigate the nature and formation processes of these layers in this particular area of the coffin.

Thirty-three archaeological microstratigraphic units were identified using soil micromorphology and classified into eight categories of deposit, DT1–8 (Table 3, Supplement 2). The classification of microstratigraphic units provides a clear understanding of depositional and post-depositional processes as a result of both disturbance as a result of the intervention, and chemical weathering induced by the decay of the body. The micromorphology results have fed into the construction of the matrix to refine the stratigraphic sequence and formation processes within the grave (Fig. 5). Twelve geological microstratigraphic units were identified and have been classified according to depositional processes that relate to the variable size and hydrology of Lake Neusiedl (Table 4), the extent of which reached Weiden during the Holocene (Hicke, 1987: 14).

3.2. Deposit type classifications of microstratigraphic units

Deposit type 1 (DT1) classifies ambiguously units 250/4, 454/11, and 592/17 as re-deposited substrate sediment, as they slightly differ from the other grave fills (DT2, DT3a, and DT6) by their absence collapsed vughs, and dusty impure clay coatings (Table 3). DT2 categorises grave fill (250/3; 251/28), at the surface that shows increasing pedogenesis towards the surface of the unit below a stone associated with the pit for the upper individual.

DT3a classifies sediment that has been used as fills (250/2) the intervention pit (470/2; 366/6; 454/12; 451/14; 364/25; and 471/26). The fill units are dark brown (PPL)/dark orange/red brown (XPL) in color, which is a lighter mid-brown (PPL) in the lower unit towards the base (642/20). The color is most probably due to iron, organic staining, and organic inclusions as indicated by the presence of inclusions such as charred wood (470/2), and ferruginous organic tissue, occurring in all fills. Several units contain a potential 'protein' substance (that may be chitin or keratin) or coprolite fragments (Shillito et al., 2011) (250/2; 451/14), and 364/25 contains fragments of decayed bone (Fig. 8). All fill units contain vughs or collapsed vughs, which can be indicative of trapped air and moisture in mass movements of sediment (Fedoroff et al., 2010: 641–642), which could include dumping processes; vughs are irregularly-shaped voids (or pore spaces) in the microstructure of a sedimentary unit, which break-up the continuity of fine material (Bullock et al., 1985: 43, 46; Stoops, 2003: 65). This sediment shares similar sediment properties and inclusions with the topsoil reference sample, 556/G12 (Table 4) and could represent the early Bronze Age topsoil being used during backfilling.

DT3b classifies 189/29 and 226/30, which are fills from the upper individual and located beneath the body. These microstratigraphic units are distinctive from the other grave fills, DT3a, as they contain sediment attributes that could be specifically attributed to their close proximity of the upper individual (Lang, 2014), such as abundant iron nodules, 20%, the greatest abundance of bone fragments, 10% (Fig. 7), needle-like calcitic infillings (Durand et al., 2010: 160), where interestingly the area below the cranium has been identified as an area for processes relating to calcite mobilisation and sedimentation (Kutterer et al., 2014a, 2014b: 181), and mesofaunal activity, which has created fine crumb peds (Table 3).

The dispersal of clays and silts is most prolific in the fill deposits, DT3a, and in those deposits that are associated with the disturbance to the underlying substrate, DT4, SE106 (Tables 3 and 4). Translocation of clay and silty clay particles is influenced by factors related to water flow, chemical conditions and energy and gravity. Movement can occur under any kind of climate, although temperate environments provide the best evidence (Courty et al., 1989). The formation of dusty impure clay coatings can be evidence of dumping under wet conditions due to turbulent hydraulic conditions and the rotational movement of sediment, often associated with the disturbance caused by trampling

Table 3

Summary of micromorphological descriptions and classifications of the archaeological samples, object 229, Weiden am See.

Sample identification					Formation processes			Composition of inclusions				Principal post-depositional alterations		
Deposit type number	Deposit type	Sample	Unit number	Strat unit	Thickness on slide (cm)	Bedding	Key sediment attributes	Rock and mineral	Building materials and sediment aggregates	Bioarch	Organic/plant	Chemical weathering	Pedogenesis	Bioturbation
DT1	Redeposited substrate	250	4	SE1/SE2	1.2–3.2	Massive	Variable particle size: clay/silt loam/sandy clay. Unsorted. Calcareous fine material. Embedded, and embedded and linked and coated related distribution. Inclusions show haphazard deposition.	Predominantly quartz (15–40%), calcite (5–20%), muscovite (5–30%), and biotite (5–10%).	Aggregates of darker soil (10%) in unit 4.	None	Ferruginous organic tissue (5%).	Iron, Manganese, Calcite coatings	Development of sub-angular blocky peds	Mesofaunal
		454	11	SE15	3.5–4.0	Massive								
		592	17	SE7	0.1–0.6	Massive								
DT2	Fill at surface	250	3	SE1/SE2	0.4–3.2	Massive	Sandy clay loam. Unsorted. Stippled b-fabric. Embedded and coated related distribution. Inclusions show haphazard deposition. Unit 28 has vughs and collapsed vughs.	Predominantly quartz (40%) with a few (<5%) mica and calcite minerals.	Aggregates of marl sediment (20%).	Bone (<5%), suspected protein (<5%), unit 3 only	Ferruginous organic tissue (10%), unit 3, charred wood <5%, unit 28.	Iron, calcite coatings	Development of sub-angular blocky peds, particularly in upper 1.2 cm 3 cm on right-side of the slide (upper 2.0–2.5 cm): fine, sub-angular blocky peds, partially accommodated, moderately to strongly developed; lower 1.5–2.0 cm sub-angular blocky peds that are accommodated and weakly developed. Remaining left-side has accommodated SA blocky ped, weakly developed.	Mesofaunal and root
		251	28	SE2	3.8–4.0	Massive								
DT3a	Fill	364	25	SE2/SE3	3.5–4.0	Massive	Variable particle size: silt loam/sandy silt loam/sandy clay loam/loamy sand/sandy clay. Unsorted. Mosaic speckled b-fabric/stippled b-fabric. Embedded and coated, and linked and coated related distribution. Inclusions show haphazard deposition. Vughs and collapsed vughs, 5–10%.	Predominantly quartz (20–50%), muscovite (5–15%), and biotite (5–15%).	Aggregates of marl sediment (10–30%). Aggregate of earthen building material, unit 2 (5%).	Bone, unit 25 (<5%), suspected protein (5–10%).	Ferruginous organic tissue (5–20%).	Dusty impure clay coatings, Iron, Manganese, Calcite coatings, Organic staining (units 6 & 25).	Development of sub-angular blocky peds (unit 12)	Mesofaunal
		366	6	SE2/SE3	0.2–4.0	Massive								
		451	14	SE7	3.2–4.0	Massive								
		454	12	SE7	4.0–4.9	Massive								
		470	2	SE7	1.5–1.8	Massive								
		471	26	SE7	0.4–1.2	Massive								
DT3b	Fill (upper burial)	189	29	SE1	2.5–2.8	Massive	Sandy clay loam/loamy sand. Unsorted. Stippled speckled b-fabric. Embedded and coated related distribution. Inclusions show haphazard deposition. Complex microstructure inc vughs.	Predominantly quartz (30%), plagioclase (20%), muscovite (5–10%), biotite (5–10%), calcite (5–10%).	Aggregates of marl sediment (20%), unit 29.	Bone (10%), suspected protein (5%).	None	Abundant iron nodules, calcite coatings, needle-like calcite infillings.	Fine crumb peds	Mesofaunal
		226	30	SE1	2.4–2.5	Massive								

DT4	Geology	470	1	SE106	0.4–0.6	Massive	Variable particle size: silt loam/sandy clay Unsorted, except unit 1 & 33 are moderately sorted fine sands, and unit 27 has bimodal sorting. Marl fine material. Variable related distribution (embedded linked and coated, and intergrain aggregate). Bridged microstructure. Inclusions show haphazard deposition.	Predominantly quartz (30–60%), calcite (5–15%), muscovite (5–20%), and biotite (5–15%).	Aggregates of darker soil (10%).	None	Ferruginous organic tissue (5–10%)	Dusty impure clay coatings, Iron, Calcite coatings (10–>25%), Organic staining (units 18 & 19).	None	Mesofaunal
		471	27		0.4–1.2	Massive								
		592	18		1.6	Massive								
		592	19		0.6	Massive								
		642	22		0.2–1.4	Massive								
669	33	2.2–2.8	Microlaminated											
DT5	Wind/water-laid sediment	450	24	SE9	1.1–1.6	Massive	Loamy sand/sandy clay loam particle size. Unsorted. Mosaic specked b-fabric. Linked and coated, and embedded and coated related distribution. Inclusions show haphazard deposition. Vughs, 10%. Variable particle size: silty clay loam/silt loam/sandy silt loam/loamy sand. Moderately sorted or bimodal sorting (moderately/well sorted silt and unsorted sand). Stippled speckled and/or stippled striated b-fabric. Embedded and linked and coated related distribution. Inclusions show haphazard deposition. Vughs, 5–10%.	Predominantly quartz (30–50%), calcite (5–10%), muscovite (5–20%), biotite (5–20%), with occasional plagioclase <10%.	Aggregates of marl sediment (10–20%).	Suspected protein, units 24 & 31 (<5%).	Ferruginous organic tissue (5–10%). Charred wood (5%) and amorphous organics (10%), unit 24.	Dusty impure clay coatings, Iron, Manganese, and Calcite coatings (units 16 & 21), Organic staining (units 16, 24, 31 & 32).	Development of sub-angular blocky peds (units 15, 16, 24, 31 & 32)	Mesofaunal. Unit 31 has been mixed with marl and sand from unit 33 (DT4).
		642	21		SE9	0.5–0.6								
		591	15	SE8	1.2	Massive								
			16	SE9	2.8	Massive								
		642	20	SE9	0.4–1.2	Massive								
		669	31	SE9	0.5–1.0	Microlaminated								
			32	SE9	0.5	Microlaminated								
DT6	Redeposited grave fill	310	5	SE2/SE3	5.7	Massive	Sandy clay/sandy clay loam. Unsorted. Marl fine material. Embedded and coated related distribution. Inclusions show haphazard deposition. Vughs and Collapsed vughs, 15%. Variable particle size: clay/silt loam/sandy clay/sandy clay loam/sandy silt loam. Bimodal sorting (moderately sorted silt and unsorted sand). Marl fine material. Embedded, and embedded and linked and coated related distribution. Inclusions show haphazard deposition. Vughs, 5%	Predominantly quartz (20–50%), calcite (5–10%), muscovite (5–20%), and biotite (5–10%).	Aggregates of darker soil (10–20%).	None	Ferruginous organic tissue (<5%), not unit 10	Dusty impure clay coatings, Iron, Manganese, Organic staining (except unit 8).	Development of sub-angular blocky peds (unit 10)	Mesofaunal
		451	13		SE7	0.1–0.4								
			8	SE2/SE3	0.7–1.7	Massive								
		311	10	SE2/SE3	1.6–2.8	Massive								
		366	7	SE2/SE3	3.2–3.9	Massive								
DT7	Re-worked microstratigraphy	311	9	SE3	3.9–4.9	Massive	Loamy sand/sandy clay loam particle size. Unsorted. Stippled b-fabric and isotropic. Embedded and coated, and linked and	Predominantly quartz (20%), muscovite (10%), with a few (<5%)	Aggregates of marl sediment (40%).	Suspected protein (<5%).	Ferruginous organic tissue (<5%).	Dusty impure clay coatings, Iron, Manganese,	None	Mesofaunal

(continued on next page)

Table 3 (continued)

Sample identification					Formation processes			Composition of inclusions				Principal post-depositional alterations		
Deposit type number	Deposit type	Sample	Unit number	Strat unit	Thickness on slide (cm)	Bedding	Key sediment attributes	Rock and mineral	Building materials and sediment aggregates	Bioarch	Organic/plant	Chemical weathering	Pedogenesis	Bioturbation
DT8	Original grave fill	450	23	SE5	0.1–1.7	Massive	coated related distribution. Inclusions show haphazard deposition. Vughs, 5%. Clay/silty clay particle size. Bimodal sorting (moderately sorted silt and poorly sorted sand). Calcareous fine material. Embedded and coated. Inclusions show haphazard deposition. Vughs, 10%.	feldspars, biotite, and calcite minerals. Predominantly quartz (50%), muscovite (20%), feldspars (10%), biotite (10%), and calcite minerals.	None	None	None	Organic staining. Dusty impure clay coatings, Iron.	None	Mesofaunal

processes in external areas (Courty et al., 1989; Shillito and Ryan, 2013). Chemical alterations and changes in the redox conditions (Brammer, 1971; French, 2003) associated with organic decay (Banerjea et al., 2015b) can lead to the dispersal of silt and clay particles and can be highly localised.

DT4 classifies units of the underlying substrate (470/1, 592/18, 592/19, 642/22, 471/27, and 699/33, Fig. 7) with sediment attributes and mineral inclusions that are comparable with the geology horizon SE106, which includes microstratigraphic units G9, G10, and G11 (Table 4). The sand components are cemented, evident by an embedded and linked and coated related distribution, within the calcareous fine material. The linked and coated related distribution shows that the

fine calcareous material has dispersed to form bridges between the sand components. These units may have formerly been a series of 'pendant' formations (Durand et al., 2010: 154–157), which have now been disturbed by root activity. The genesis of pendant formation is accompanied by changes in the chemical composition, particularly with magnesium rates. In temperate regions, pendant formation seems to be controlled by the progression of weathering during which the carbonates are destabilised and not associated with a simple continuous carbonate accretion (Durand et al., 2010: 156); calcite hypo-coatings (Durand et al., 2010: 158–159) also occur. The carbonates may have also been destabilised due to the decay of a body part/tissue or other organic remains in this area (Kutterer et al., 2014a, 2014b: 181), as these

Table 4

Summary of micromorphological descriptions and classifications of the geological samples, Weiden am See.

Interpretation	Sample	Unit number	Key descriptive attributes	Composition	Post-depositional alterations
Topsoil with anthropogenic inclusions	556	G12	Sandy clay loam. Unsorted. Stippled speckled b-fabric. Complex microstructure with sub-angular blocky peds moderately-strongly developed, partially-unaccommodated, chambers 10%, and vughs 2%	Quartz 30%, Muscovite 5%, Microcline 5%, Plagioclase 10%, Calcite 20%, Manganese 5%, Iron 10%, Flint 5%, Limestone 10%, Aggregates of clay sediment 10%, Unburnt bone 5%, Shell 5%, Charred wood 10%	Sub-angular block ped microstructure. Mesofaunal bioturbation 20%. Calcitic earthworm granules 5%, Calcitic coatings 10%. Calcitic infillings 5%
Reworked marl	527	G1	Silty clay. Bimodal: moderately sorted silt, poorly sand. Complex microstructure including vughs, 10%	Quartz 50%, Plagioclase 15%, Calcite 5%, Muscovite 5%, Iron 5%, Sediment aggregates of topsoil 15%, Organic tissue 5%	Crumb microstructure. Abundant mesofaunal bioturbation, 20%. Rare, mesofaunal casts 2%.
Marl	530	G2	Silty clay. Bimodal: moderately sorted silt, poorly sand. Crystallitic b-fabric. Complex microstructure including vughs, 10%	Quartz 55%, Plagioclase 15%, Microcline 5%, Calcite 5%, Muscovite 5%, Iron 10%, Manganese 5%	Abundant mesofaunal bioturbation, 15%.
Waterlaid sediment-low energy	533	G3	Silt loam/silty clay loam. Well sorted silt. Mica fragments are moderately oriented aligned parallel to the basal boundary. Microlaminations.	Quartz 30%, Biotite 30%, Muscovite 15%, Calcite 5%, Iron 10%, Manganese 10%, Organic tissue 5%	Clay translocation, 2% Mesofaunal bioturbation, 5%
Waterlaid sediment-higher energy than G3		G4	Loamy sand/sandy silt loam. Bimodal: well sorted silt, moderately sorted sand. Silt-sized mica fragments are moderately to strongly oriented aligned parallel to the basal boundary. Complex microstructure: Vughs 10%, Simple packing voids, Bridged. Microlaminations.	Quartz 30%, Biotite 30%, Muscovite 10%, Plagioclase 10%, Calcite 5%, Iron 10%, Manganese 5%, Shell 5%, Organic tissue 2%, Charred wood 2%	Clay translocation, 2%
Waterlaid sediment-lower energy than G4		G5	Silt loam/sandy silt loam. Bimodal: well sorted silt, moderately sorted sand. Silt-sized mica fragments are moderately oriented aligned parallel to the basal boundary. Complex microstructure including Vughs 2% Vesicles 2%. Microlaminations.	Quartz 30%, Biotite 30%, Muscovite 10%, Plagioclase 5%, Calcite 5%, Iron 10%, Rounded sediment aggregates of marl 10%	Clay translocation, 2% Mesofaunal bioturbation, 20%
Marl	536	G6	Silty clay. Well sorted silt in clay matrix. Silt quartz grains are moderately oriented. Crystallitic b-fabric. Complex microstructure including Vughs 20% Vesicles 10%	Quartz 45%, Muscovite 20%, Plagioclase 5%, Calcite 10%, Iron 10%, Manganese 5%,	Mesofaunal bioturbation, 5%
Marl- higher energy than G6		G7	Sandy clay. Unsorted. Inclusions are unoriented, unrelated, random, and unpreferred. Crystallitic b-fabric. Complex microstructure including Vughs 10% Vesicles 5%	Quartz 50%, Muscovite 10%, Plagioclase 5%, Calcite 10%, Limestone 10%, Sandstone 5%, Iron 5%, Manganese 5%,	Mesofaunal bioturbation, 10%
Marl		G8	Silty clay. Well sorted silt in clay matrix. Silt quartz grains are moderately oriented. Crystallitic b-fabric. Complex microstructure including Vughs 20% Vesicles 10%	Quartz 80%, Muscovite 5%, Biotite 5%, Iron 5%, Manganese 5%,	Mesofaunal bioturbation, 5%
Lake edge Wind-blown sands	541	G9	Loamy sand. Bimodal: moderately sorted silt; poorly sorted sand. Mica fragments are strongly oriented aligned parallel to the inclined basal boundary. Crystallitic and mosaic, speckled b-fabric. Complex packing voids and vughs.	Quartz 30%, Biotite 10%, Muscovite 10%, Microcline 5%, Plagioclase 10%, Calcite 20%, Iron 5%, Manganese 5%, Shell 10%, Charred wood 2%	Mesofaunal bioturbation, 10% Calcitic coatings 10% Calcitic infillings 10%
Lake edge fluvial sands affected by frost action		G10	Sand/loamy sand. Moderately sorted sand. Crystallitic and mosaic, speckled b-fabric. Complex packing voids and vughs. Lenticular platy peds that are strongly oriented aligned parallel to inclined basal boundary (Van Vliet-Lanoë, 2010: 83–90).	Quartz 30%, Biotite 20%, Muscovite 10%, Microcline 5%, Plagioclase 10%, Calcite 20%, Manganese 5%, Aggregates of clay sediment 10%	Mesofaunal bioturbation, 5% Calcitic coatings 10%
Lake edge, wind-blown sands affected by frost action		G11	Loamy sand. Bimodal: moderately sorted silt; poorly sorted sand. Crystallitic and mosaic, speckled b-fabric. Compound packing voids and bridged microstructure. Lenticular platy peds that are strongly oriented aligned parallel to inclined basal boundary (Van Vliet-Lanoë, 2010: 83–90).	Quartz 50%, Biotite 5%, Muscovite 10%, Microcline 5%, Plagioclase 20%, Calcite 20%, Manganese 5%, Aggregates of clay sediment 10%	Calcitic coatings 10%

carbonate pedofeatures are more prolific (10–25%) beneath the grave than in the adjacent geological profile (10%). These units (DT4) do not contain any bone fragments or other anthropogenic inclusions, although there are inclusions of the ferruginous organic tissue, which may have been reworked into these units from the fills.

DT5 classifies deposits of water/wind laid sedimentation (591/15, 591/16, 642/20, 642/21, 450/24, 669/31, and 669/32 Fig. 7). 591/15 is moderately sorted sand, and 591/16 has a moderately sorted silt component. Sediments that have a better degree of sorting tend to be a result of processes such as wind or water deposition, rather than mass movements of sediment such as colluvium, which tends to be more poorly sorted (Goldberg and Macphail, 2006). Vughs within 591/16, 669/31, and 669/32 indicate the presence of moisture, and suggests that this sediment may have been deposited under wet conditions. 642/21, 669/31, and 669/32 have a stippled speckled, and striated b-fabric from clay depositions, and there are microlaminations of silt loam/silty clay loam sediment (Fig. 7), which are indicative of low energy sedimentation processes over time (Goldberg and Macphail, 2006). The microlaminations have been reworked by bioturbation, particularly in 642/20, 642/21, and 669/31, although the microlaminations are still visible despite this (Fig. 7). Fragments of ferruginous organic tissue, 5%, occur in all these units.

DT6 classifies sediment of the original grave fill that has been re-deposited (310/5, 366/7, 311/8, 311/10, and 451/13). 310/5 and 366/7 are similar in color to those in DT1 and DT8, but 310/5 in particular has a coarse particle size and is unsorted in comparison with the original grave fill, DT8. The occurrence of collapsed vughs, as also observed in the fills, DT3, can be indicative of trapped air and moisture in mass movements of sediment (Fedoroff et al., 2010: 641–642), which could include dumping processes. Unlike the geological marl sediments, the fills within the grave do not contain vesicles (Tables 3 and 4), which suggests that these have been collapsed or destroyed by the redeposition of this sediment. Vesicles are smooth-walled, simple-curved voids attributed to the incorporation of air bubbles in near-surface horizons, and have also been observed in the puddled layer of paddy soils (Stoops, 2003: 64–65).

All units, with the exception of 311/8, contain fragments of ferruginous organic (plant) tissue, although there are fewer than other deposit type categories, <5%. 310/5, 366/7 and 311/10 contain sediment aggregates, 20%, of brown organic, 'fill-like' fabric, which are similar to the present day topsoil (Table 4; Fig. 4), and could represent aggregates of the early Bronze Age topsoil that have been incorporated during backfilling, as suggested for DT3a.

311/9 has been assigned a separate deposit type, DT7, due to the severe re-working of what appears to have been three individual units. There are sub-rounded aggregates of both organic 'fill-like' sediment and sediment similar to DT4, the calcareous sedimentation, 0.5 mm–0.7 cm. It seems that an organic lens had previously formed between two sand lenses into which calcareous fine material precipitated, in a similar way to DT4. This unit contains a potential 'protein' substance (that may be chitin or keratin) or coprolite fragments (Shillito et al., 2011) (Table 3).

DT8 categorises a single deposition of original grave fill, 450/23. This unit is similar in particle size, sorting, and color to those in the re-deposited substrate, DT1. The occurrence of vughs, as also observed in the fills, DT3, could indicate dumping processes. There are no aggregates of different sediment, bone, 'protein' substances/coprolite fragments, or organic remains within this unit, and it shares comparable sediment attributes with the marl sediment, particularly microstratigraphic unit G2 within the adjacent geological profile (Table 4; Fig. 4).

3.3. Interpretation of results: formation processes Weiden am See 2013/object 229

The formation of the archaeological evidence of Weiden am See Object 229 includes short and long-term processes (Fig. 9). After the deposition of the coffin (SE11–14, SE16) that contained the body of individual 1 (male, 25–35 years; group 4) the pit was filled, represented in 450/23 (SE3, SE5, SE15). The decay of the body of individual 2 and also of the coffin started. Grave fill above the coffin (SE3, SE5, SE15) was compacted due to natural processes (gravity, weather) and clay

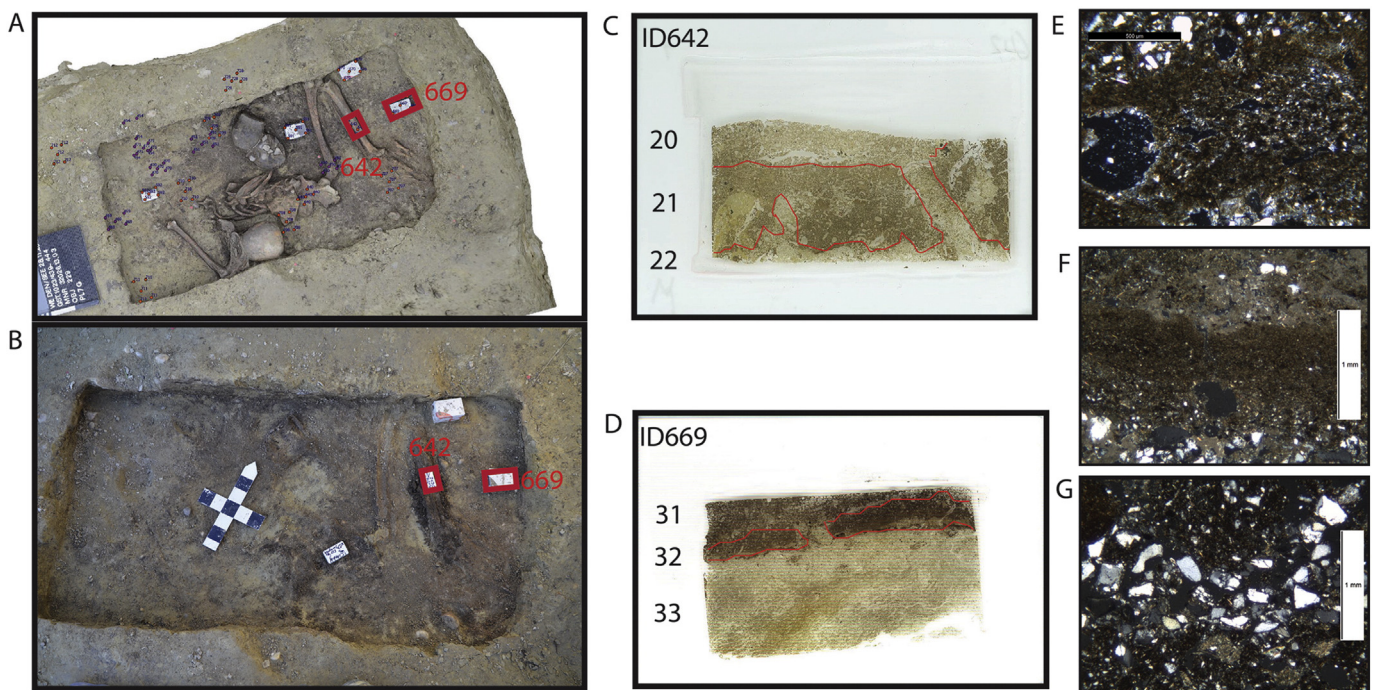


Fig. 7. Location of micromorphology samples 642 and 669 (a and b); scan of slides 642 and 669 with associated microstratigraphic units (c and d); and units of wind or water-laid sediment in 642/21 (e), 669/32 (f), and reworking of unit 669/31, where sand from 669/33 has been brought up into a channel within 669/31 (g).

soil particles were washed towards the bottom of the grave, with some particles entering the coffin through its top (SE6) – which was unlikely to have been absolutely tight. Soil particles may also have got into the coffin during the funeral (wind-blown). Inside the coffin, these soil particles and water perhaps mixed with ground water and liquids from decay of the body during putrefaction (Pinheiro, 2006), leading to the formation of predominately silt loam lenses; these are moderately sorted, or have a bimodal sorting with moderately to well sorted silt, and unsorted sand (SE9) at the bottom of the coffin and a more sandy layer, 591/15 (SE8) on top of it. These silt and fine sand deposits accumulated forming a series of lenses, which have been categorized as DT5 (Fig. 642 & 669 DT5 Fig. 7), in the area between the femora and trunk, possibly because a separate space was created within the coffin due to the presence of the body and possibly due to irregularities in the base of the coffin.

When the grave was reopened, a pit was dug in the west end of the grave and the coffin was broken into. Both the cranium and mandible as well as skeletal parts from the right side of the trunk and upper limbs had been moved and were no longer in anatomical connection upon discovery. It can be seen that parts of the body were still articulated at that time, e.g. the left scapula and humerus, while other parts had disarticulated already (e.g. upper vertebrae, the mandibula and cranium). There was hardly any bone damage (breakage) indicating that the hollow space of the coffin was still intact at that stage. The reopening pit was immediately refilled (SE7), represented by units that are classified in DT1, DT3a, and DT6, forming a heap in the hollow space inside

the coffin. Material may have been dug out during the intervention, piled up on the side and then put back in as backfill during the refilling of the intervention pit. However, parts of the original grave fill (SE3) slumped towards the reopening pit, represented by units that are classified in DT3a, DT6, and DT7 (Table 3), and less than half of the grave was filled with the original grave fill (Fig. 6). Also the refill of the reopening pit would have been compacted due to natural processes such as under the weight of the sediment. It appears that after an initial quick refill of the bottom of the reopening pit the top of the reopening pit may not have been refilled immediately. There is an accumulation of pottery and daub on the bottom of SE2 in the area surrounding the 'funnel' of SE3A. At a later stage, a pit was dug into the top of the grave, which was left exposed for some time (a season or so), as indicated by units classified as DT2. Large stone blocks were set into the pit and partly covered with dirt, which formed an uneven surface on which the body of individual 1 (probably male, adult) was placed on the left side with the lower limbs flexed. There is no evidence for any coffin or other structure surrounding the body, but there was some hollow space for the body to move from its original position to a prone (face-down) one during decay.

Radiocarbon measurements of the skeletal remains of individual 1 and 2 suggest a timeframe of 10–40 years for the duration of the formation of the archaeological evidence. Two batches of samples (individual 1: right and left femora, individual 2: part of the mandible, left femur) were measured which produced basically identical results (Fig. 10). Calibration of C14 measurements shows 95%

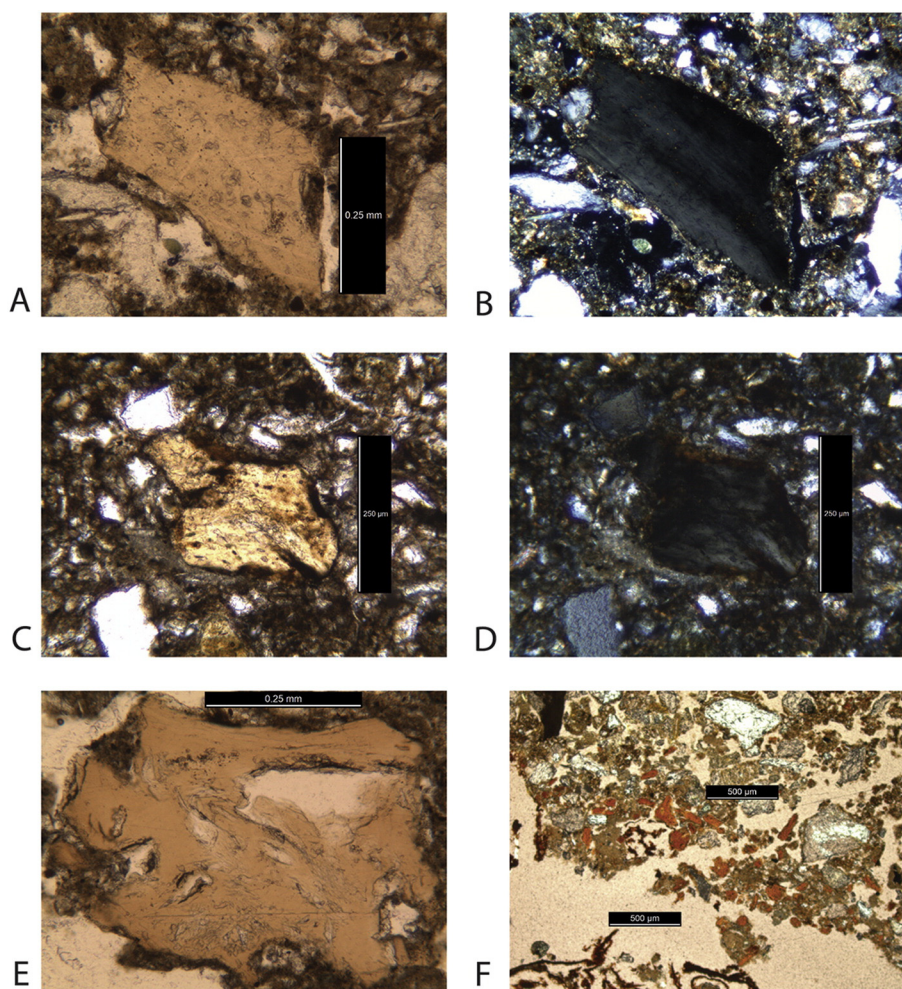


Fig. 8. Photomicrographs of bone fragments within 189/29, ppl (a), xpl (b), 364/25, ppl (c), xpl (d), 226/30, ppl (e), and fragments of the possible protein substance within 471/2 (f).

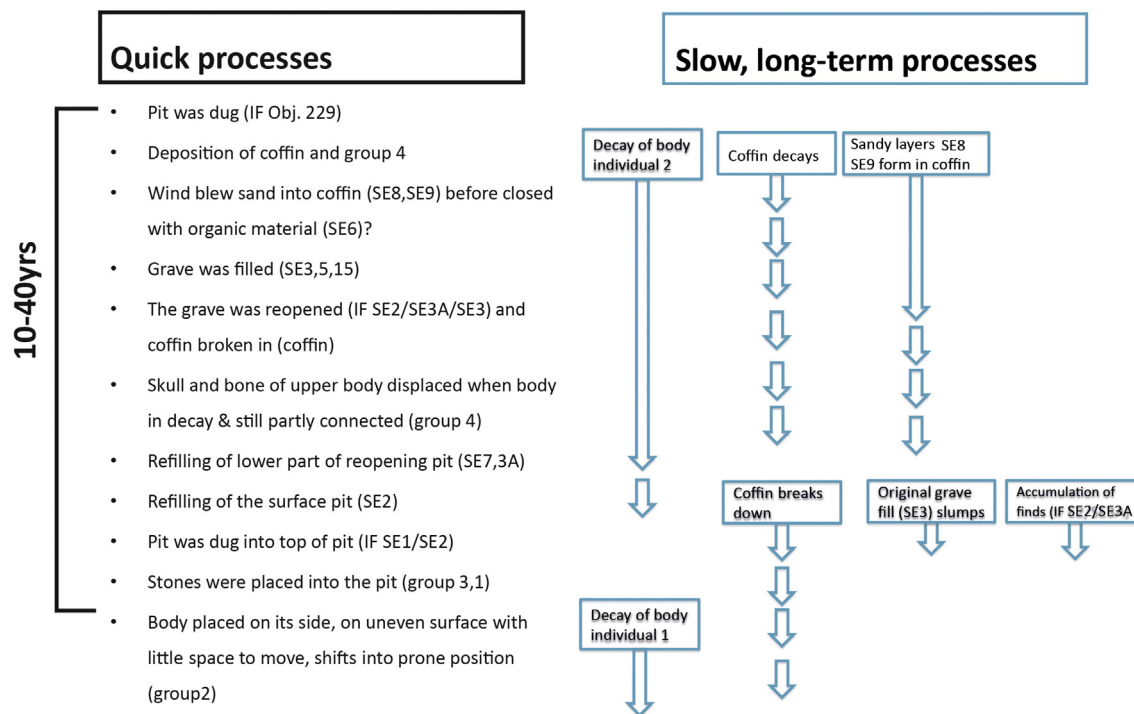


Fig. 9. Formation processes at Weiden am See 2013/obj. 229.

probability of 1970–1850 BCE calendar years for individual 2 and 1780–1660 BCE for individual 1 (Reimer et al., 2013). This would suggest that a time period of 150 to 250 years passed between the deposition of individual 2 at the bottom of the grave and the burying of upper individual 1. However, the mathematics of calibration and the normalization process have been shown to have flaws, which are particularly relevant for case studies with relatively small sample sizes (Weninger et al., 2015).

Comparing the paired C14-ages of individual 1 and 2 with the relevant INTCAL13 raw data sets shows that there is another solution where the two individuals were buried only 10–40 years (min/max) apart in time (Fig. 10). The existence of this solution only becomes apparent when the calibration is performed by visual means, based on the relevant INTCAL13 raw data sets. We expect that it has been this shorter time interval and the shifting of left lower limb of individual 1 downwards may have been caused by the collapse of the coffin and consequent subsiding of sediment underneath individual 1.

4. Discussion

Micromorphological analysis of undisturbed sediment samples from Weiden am See object 229 answered a series of key research questions relating to deposit characterization and formation processes associated with the construction of and intervention in the grave, and the time-scales of these events (see Sections 4.1–4.4), in order to understand fully the taphonomy of this reopened grave. This microstratigraphic analysis also resulted in important additional findings relating to the depositional conditions, effects on and movement of sediment as a result of the decay of the body, and the identification of new microstratigraphic units not previously observed during excavation (Sections 4.5–4.7).

4.1. Disturbed and undisturbed areas distinguished

At excavation, it was not possible to identify the extent of the intervention pit. Categorizing microstratigraphic units as either 'fill' or 're-

deposited fill' showed that the disturbed area in the grave pit was much larger than the 'funnel' seen at excavation (Fig. 6) because of slumping processes after the reopening. Only one unit (450/23) was classified as grave fill (Table 3), and this distinction was in some cases not as clear. The resulting model is that after the reopening, parts of the original grave fill were slumping into the reopening pit (310/5, 311/8,7) and the original extent of the reopening pit was not preserved in the archaeological record.

4.2. Stratigraphic units distinguished and characterized

Micromorphological analysis was instrumental in characterizing and categorizing fills within this grave and their depositional processes. More specifically, it has identified the sediment attributes of fills inside and outside of the coffin area, distinguished the original grave fill from that sediment, which had been used to backfill the intervention pit, and identified differences between the fills surrounding the upper individual, the intervention pit, and in the coffin. In particular, micromorphology identified the aqueous depositional pathways of sediment within the lower burial (DT5; SE9), at the base of the coffin that may, in part, relate to the decay of the body.

The identification of microscopic inclusions, which were not identified during excavation, within microstratigraphic units enabled them to be quantified and examined within their depositional context. For example, fragments of decayed bone occur most abundantly (10%) within units directly beneath the body of individual 1 (189/89, 226/30), specifically the humerus and tibia (Fig. 8), and charred wood, which, as examination of the geological profile has shown (Table 4), may have been reworked throughout the profile by mesofauna, or transported by water as a result of Holocene expansion of the lake (Hicke, 1987). A 'protein' substance (that may be chitin or keratin) or coprolite fragments (Shillito et al., 2011) (Fig. 8) has been identified in many units from the base of the coffin, which may result from the decay of the human body individual 2 (Fig. 9), and is a strand of further analysis.

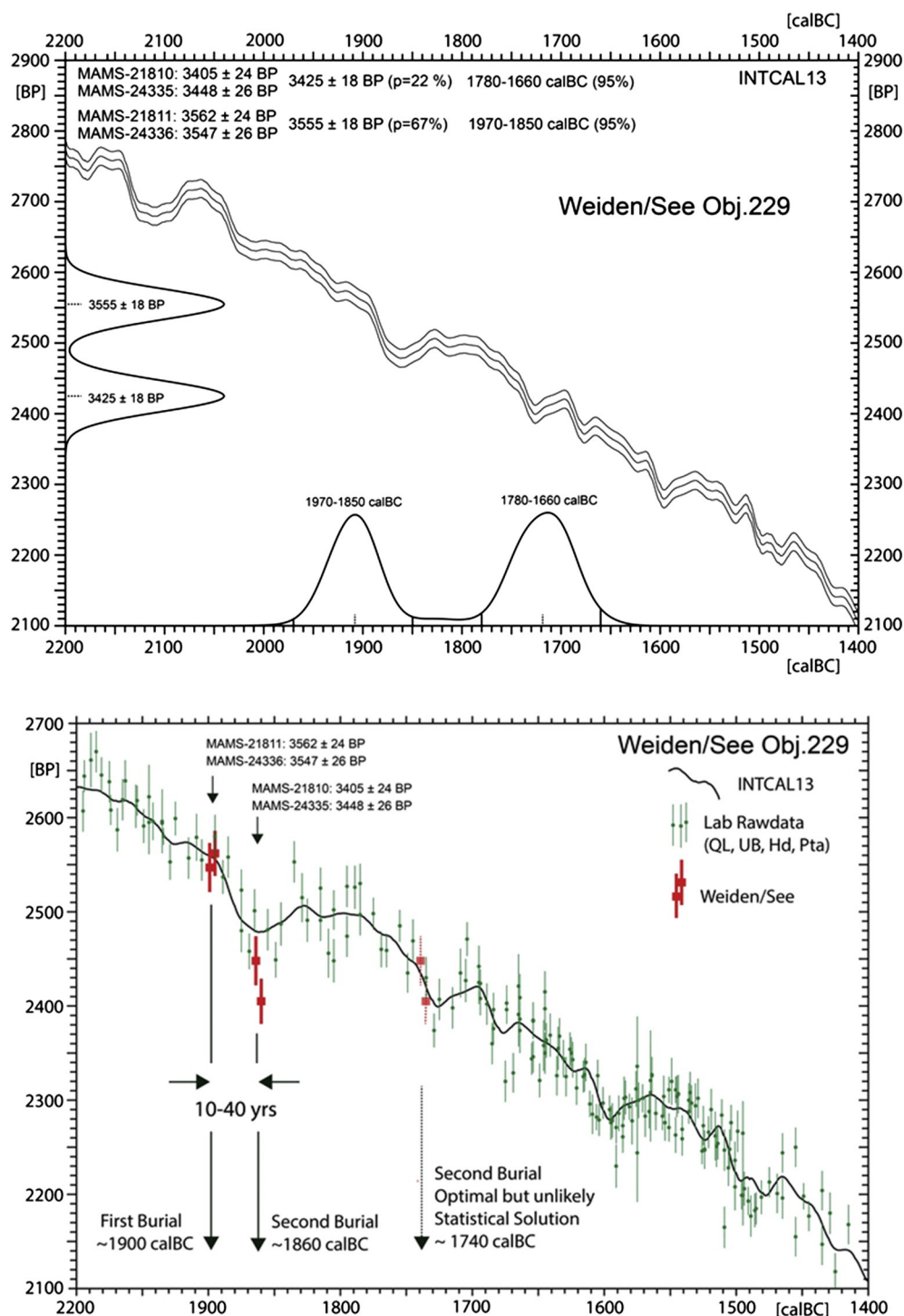


Fig. 10. Results of radiocarbon measurements: Top: 2-D Dispersion Calibration of ^{14}C -Ages (weighted averages) from Weiden/See. Bottom: Visual wiggle-matching of paired ^{14}C -ages of individual 1 and 2 from Weiden/See 2013, Object 229. Graphic produced with CalPal-Software using two dialogs in combination: Gaussian Monte Carlo Wiggle Matching and Reservoir Explorer.

4.3. Examine stratigraphic interfaces

The refilled material of a reopened grave can be very heterogeneous and the result of different episodes. At excavation it can be difficult to distinguish between boundaries between different types of fills that were part of one refill event and surfaces that were the result of human intervention (pit cut). Sample 250/3 from the surface of SE2 (which is the bottom of the pit into which individual 1 was buried)

shows evidence for exposure: the upper 1.2 cm of the unit had been reworked more and show evidence of surface weathering, although it is difficult to state the timescale or duration of this phenomenon.

4.4. Timescales of sediment deposition

At the very bottom of the grave, where the coffin had been broken through, there was no evidence of slow sedimentation after the

reopening, but evidence of various episodes of dumping of sediments (samples 592/17) and 470/2 and 454/12). Unit 17 is a lump of substrate material that entered the coffin at/or after the reopening. Inside the coffin, two layers were found of moderately sorted sand formed by slow aqueous sedimentation (591/15, 16; 642/20; 642/21; 450/24; 669/31, 32, Fig. 7) related to groundwater and liquids in the coffin (see above).

4.5. Post-depositional changes of sediments

Wind/water-laid sediment (DT5) formed by fine particles that had originally entered the coffin through coffin boards, or may have been blown into the coffin if left open for some time, were mobilized with finer clay sediment, possibly as a result of fluids from the decay of the body (Pinheiro, 2006). This material accumulated at the base of the coffin where it also entered the pots (559, 638, 637) (Table 3). The Lake Neusiedl area is a particularly windy area (presently used for wind-surfing); the local excavation team observed that a substantial layer of fine, wind-blown sand can accumulate inside a grave within a day.

Micromorphological analysis has identified areas within the grave that show evidence for greater bioturbation, such as at the base of the coffin, particularly in 669/31 where mesofauna have reworked organic fragments and substrate from unit 33 (SE106) into their burrows, and in areas of the upper individual, specifically within samples directly under the body (189/29; 226/30) in the form of iron nodules, needle-like calcite infillings of voids, and fine crumb microstructure from mesofaunal activity, and prolific pedogenesis at the surface of the pit for the deposition of individual 1250/3; 251/28.

4.6. Conditions of the depositional environment

Vughs and collapsed vughs, and dusty impure clay coatings in fills and re-deposited fills (Table 3) can be interpreted as evidence of dumping under wet conditions, particularly in the refill of the reopening pit (SE2, 3A, 7 slides 366/6364, 454/12, 470/2), and the former, particularly collapsed vughs (DT2, DT3a, DT6) evidence of mass movement of wet sediment, i.e. the use of sediment as grave fill (and inside the coffin, with the sandy wind/water-laid layers, represented by layers 451/14).

4.7. Refine stratigraphy – identification of key micro-stratigraphic units

Microstratigraphic analysis identified and characterized the formation processes of microstratigraphic units classified as DT5, wind and water-laid sediment, by the identification of several aqueous depositions of microlaminations. These processes had not been identified during excavation, but microstratigraphic analysis has enabled the formation of SE9 to be interpreted.

5. Conclusions

Soil micromorphology has been demonstrated to be instrumental in interpreting the complex taphonomy of this reopened grave, and has an important role to play in future research in this area to add to the growing body of micromorphological research on graves (Kutterer et al., 2014a, 2014b; Lang, 2014; Usai et al., 2014; Macphail et al., 2013; Sandgathe et al., 2011; Huckleberry et al., 2003). Most importantly, it provides information about areas in the grave which had been disturbed or remained undisturbed and about the refilling of the grave (slow, quick). Post-depositional transformation processes (e.g. effects of decay of the body on formation of sediments) can be identified and observations at excavation can be investigated further. In general, a more precise stratigraphy and a highly detailed sequence of the formation process can be gained (e.g. after the reopening, the refilling of the grave took place under wet conditions, the surface of SE2 was exposed for some time).

In this pilot study the potential of soil micromorphology to address questions of reopened graves has been explored under special, experimental circumstances with special funds reserved for analysis of many samples. While such a time- and cost-intensive approach will not be possible for most projects, we argue that, generally, with a clear research question in mind soil micromorphology can be a great tool for the analysis of archaeological mortuary evidence, particularly to examine questions relating to the deposition of sediments during burial, the decay of the body, and later disturbance of the grave. Micromorphology may also be applied during the excavation process to answer very specific questions about the formation of single deposits, which makes sampling and analysis more time- and cost-effective. For example, in this research, although 53 archaeological micromorphology samples were collected, 17 were prepared and analyzed to answer key questions concerning formation processes when they arose).

In any case, for successful application of micromorphological studies, a close collaboration of archaeologist and micromorphologist is crucial. This ideally would start with a micromorphologist being involved in the planning of the excavation and sampling strategy and them being present at excavation, as taking samples already requires some background knowledge and experience of selecting a sample location and sample collection.

Finally, we want to emphasize the importance of the detailed recording of the samples to clearly link them to the stratigraphic sequence and to also know their precise location within a stratigraphic context, e.g. their relationship to the body and other features which may have decayed. Strategic spatial and stratigraphic sampling of every unit, for example around the body, inside and outside the coffin, and of the grave fill is necessary to fully understand complex formation processes of mortuary deposits. Additionally, the examination of the geological profile is crucial for understanding the origin and transformation of sediments within the grave.

Supplementary data to this article can be found online at <http://dx.doi.org/10.1016/j.jasrep.2016.07.003>.

Acknowledgements

This research was supported by a Hertha Firnberg Post-doctoral fellowship from the Austrian Science Fund (FWF): T595-G19 and by the Oelzelt-Newin'sche Foundation and Institute for Oriental and European Archaeology, Austrian Academy of Sciences. Many thanks go to the research group Quaternary Archaeology (OREA), the Austrian Federal Monuments Office, Department of Archaeology and the excavation team ARGE Zeitalter for support and good collaborations during excavation and beyond. We are grateful to Bernhard Weninger, University Köln for his help with the calibration of the C14 results and for the discussion of their alternative interpretation. We would like to thank the following people for their contributions to the figures: Martin Fera (Fig. 1), Nikolaus Franz (Fig. 2), Irene Petschko and Mario Börner (Fig. 3) and Seta Štuhec (Video). Thanks are extended to the following individuals: Franz Sauer, Christine Neugebauer-Maresch, Marc Händel, Norbert Buchinger, Erich Draganitz, Rod Salisbury, Petra Schneidhofer, Richard Macphail, Natalie Marini.

References

- Aspöck, E., 2005. Graböffnungen im Frühmittelalter und das Fallbeispiel der langobardenzeitlichen Gräber von Brunn am Gebirge, Flur Wolfholz, Niederösterreich. *Archaeologia Austriaca* 87 (2003), 225–264.
- Aspöck, E., 2011. Past "disturbances" of graves as a source: taphonomy and interpretation of reopened early medieval inhumation graves at Brunn am Gebirge (Austria) and Winnall II (England). *Oxford Journal of Archaeology* 30 (3), 299–324.
- Aspöck, E., 2015. '(Deviant?) burial- and post-burial treatment of bodies at the mid Anglo-Saxon cemetery Winnall II: troubles among the living or between the living and the dead?' In: Devlin, Z.L., Graham, E.J. (Eds.), *Death embodied: Archaeological Approaches to the Treatment of the Corpse*. Oxbow Books, Oxford.
- Aspöck, E., Klevnäs, A., 2011. Past 'disturbances' of graves: the reopening of graves for 'grave-robbery' and other practices (Session report, EAA 2011). *The European Archaeologist* 36, 66–70.

- Aspöck, E., Klevnäs, A., van Haperen, M., Noterman, A., Zintl, S., 2016. Grave Reopening Research. <http://reopenedgraves.eu> (accessed 14.03.16).
- Banerjea, R.Y., Fulford, M., Bell, M., Clarke, A., Matthews, W., 2015a. Using experimental archaeology and micromorphology to reconstruct timber-framed buildings from Roman Silchester: a new approach. *Antiquity* 89 (347), 1174–1188.
- Banerjea, R.Y., Bell, M., Matthews, W., Brown, A.D., 2015b. Applications of micromorphology to understanding activity areas and site formation processes in experimental hut floors. *Archaeological and Anthropological Sciences* 7, 89–112.
- Brammer, H., 1971. Coatings in seasonally flooded soils. *Geoderma* 6, 5–16.
- Bullock, P., Fedoroff, N., Jongerius, A., Stoops, G., Tursina, T., 1985. *Handbook for Thin Section Description*. Waine Research, Wolverhampton.
- Canti, M.G., 2003. Earthworm activity and archaeological stratigraphy: a review of products and processes. *Journal of Archaeological Science* 30, 135–148.
- Courty, M.A., Goldberg, P., Macphail, R., 1989. *Soils and Micromorphology in Archaeology*. Cambridge University Press, Cambridge.
- Devos, Y., Vrydaghs, L., Degraeve, A., Fechner, K., 2009. An archaeopedological and phytolitarian study of the “Dark Earth” on the site of Rue de Dinant (Brussels, Belgium). *Catena* 78, 270–284.
- Dibble, H.L., McPherron, S.P., 1991. Computers and prehistoric archaeology. *Les Cahiers de la Vallée de la Couze* 2–3, 69–73.
- Durand, N., Monger, H.C., Canti, M.G., 2010. 9 - calcium carbonate features. In: Stoops, G., Marcelino, V., Mees, F. (Eds.), *Interpretation of Micromorphological Features of Soils and Regoliths*. Elsevier, Amsterdam, pp. 149–194.
- Fedoroff, N., Courty, M.-A., Guo, Z., 2010. 27 - palaeosoils and relict soils. In: Stoops, G., Marcelino, V., Mees, F. (Eds.), *Interpretation of Micromorphological Features of Soils and Regoliths*. Elsevier, Amsterdam, pp. 623–662.
- Franz, N., Schwarzäugl, J., Tögel, A., Tögel, W., 2014. KG Weiden am See, MG Weiden am See. Mnr. 32026.14.01, 32026.14.02 I Gst. Nr. 1023/360–366, 1023/368–373, 1023/384–398, 1023/401–412, 1023/433–436, 1023/449–451, 1023/454 I Jungsteinzeit und Frühmittelalter, Siedlungen I Bronzezeit, Gräberfeld I Römische Kaiserzeit, Villa rustica I Zeitgeschichte, Befestigungen. *Fundberichte aus Österreich* 53, 173–174.
- French, C., 2003. *Geoarchaeology in Action: Studies in Soil Micromorphology and Landscape Evolution*. Routledge, New York and Oxford.
- Gé, T., Courty, M.A., Matthews, W., Watez, J., 1993. *Sedimentary formation processes of occupation deposits*. Prehistory Press, Madison.
- Goldberg, P., Macphail, R., 2006. *Practical and Theoretical Geoarchaeology*. Blackwell Publishing, Malden, Oxford and Victoria.
- Händel, M., 2010. Different excavation techniques and their stratigraphic results. A comparison of the excavations of Krems-Hundssteig 2000–2002 and Krems-Wachtberg 2005. In: Neugebauer-Maresch, C., Owen, L. (Eds.), *New Aspects of the Central and Eastern European Upper Palaeolithic - Methods, Chronology, Technology and Subsistence*. Mitteilungen der Prähistorischen Kommission, Wien, pp. 285–293.
- Hicke, W., 1987. *Hügel- und Flachgräber der Frühbronzezeit aus Jois und Oggau*. Burgenländisches Landesmuseum, Eisenstadt.
- Huckleberry, G., Stein, J., Goldberg, P., 2003. Determining the provenience of Kennewick Man skeletal remains through sedimentological analyses. *Journal of Archaeological Science* 30, 651–665.
- Klevnäs, A.M., 2007. Robbing the dead at Gamla Uppsala, Sweden. *Archaeological Review from Cambridge* 22, 24–42.
- Klevnäs, A.M., 2013. Whodunnit? Grave-robbery in Anglo-Saxon England and the Merovingian Kingdoms. *British Archaeological Reports*, Oxford.
- Klevnäs, A., 2015. Abandon ship! digging out the dead from the Vendel boat-graves. *Norwegian Archaeological Review* 48, 1–20.
- Krenn-Leeb, A., 2011. *Zwischen Buckliger Welt und Kleinen Karpaten: Die Lebenswelt der Wieselburg-Kultur*. Archäologie Österreichs 22.
- Kümmel, C., 2009. *Ur- und frühgeschichtlicher Grabraub*. Archäologische Interpretation und kulturanthropologische Erklärung. Waxmann, Münster.
- Kutterer, A., Overlaet, B., Miller, C.E., Kutterer, J., Jasim, S.A., Haerinck, E., 2014a. Late pre-Islamic burials at Mleiha, Emirate of Sharjah (UAE). *Arabian archaeology and epigraphy* 25, 175–185.
- Kutterer, A., Overlaet, B., Miller, C.E., Kutterer, J., Jasim, S.A., Haerinck, E., 2014b. Late pre-Islamic burials at Mleiha, Emirate of Sharjah (UAE). *Arabian Archaeology and Epigraphy* 25, 175–185.
- Lang, C., 2014. *The Hidden Archive of Historical Human Inhumations locked within Burial Soils*. Department of Archaeology, University of York Unpublished PhD thesis.
- Leeb, A., 1987. Überblick über die Chorologie, Typologie und Chronologie der Wieselburgkultur. In: Hicke, W. (Ed.), *Hügel- und Flachgräber der Frühbronzezeit aus Jois und Oggau*. Burgenländisches Landesmuseum, Eisenstadt.
- Macphail, R.I., 1994. The reworking of urban stratigraphy by human and natural processes. In: Kenward, H.K. (Ed.), *Urban-Rural Connexions: Perspectives from Environmental Archaeology*. Oxbow, Oxford, pp. 13–43.
- Macphail, R.I., Galinié, H., Verhaeghe, F., 2003. A future for Dark Earth? *Antiquity* 77, 349–358.
- Macphail, R., Bill, J., Cannell, R., Linderholm, J., Rødsrud, C.L., 2013. Integrated microstratigraphic investigations of coastal archaeological soils and sediments in Norway: the Gokstad ship burial mound and its environs including the Viking harbour settlement of Heimdaljordet, Vestfold. *Quaternary International* 315, 131–146.
- Matthews, W., 1995. Micromorphological characteristics of occupation deposits and microstratigraphic sequences at Abu Salabikh, Southern Iraq. In: Barnham, A.J., Macphail, R.I. (Eds.), *Archaeological Sediments and Soils: Analysis, Interpretation and Management*. University College, London, Institute of Archaeology, pp. 41–76.
- Murphy, C.P., 1986. *Thin Section Preparation of Soils and Sediments*. A.B. Academic Publishers, Berkhamsted.
- Musell® Color, 2000. *Musell® Soil Color Charts*. 2000. Cretag Mc-Beth, New Windsor, Wyoming.
- Neugebauer, J.-W., 1988. Die Nekropole F von Gemeinlebern, NÖ. Untersuchungen zu den Bestattungssitten und zum Grabraub in der ausgehenden Frühbronzezeit in Niederösterreich südlich der Donau zwischen Enns und Wienerwald. Universität Wien, Wien.
- Neugebauer, J.-W., 1991. Die Nekropole F von Gemeinlebern, Niederösterreich. Untersuchungen zu den Bestattungssitten und zum Grabraub in der ausgehenden Frühbronzezeit in Niederösterreich südlich der Donau zwischen Enns und Wienerwald. Philipp von Zabern, Mainz am Rhein.
- Neugebauer-Maresch, C., Neugebauer, J.-W., 1997. *Franzhausen: Das frühbronzezeitliche Gräberfeld I*. Ferdinand Berger & Söhne, Horn.
- Pinheiro, J., 2006. Decay process of a cadaver. In: Schmitt, A., Cunha, E., Pinheiro, J. (Eds.), *Forensic Anthropology and Medicine*. Humana Press, Totowa, New Jersey, pp. 85–116.
- Reimer, P.J., Bard, E., Bayliss, A., Beck, J.W., Blackwell, P.G., Bronk Ramsey, C., Buck, C.E., Cheng, H., Edwards, R.L., Friedrich, M., Grootes, P.M., Guilderson, T.P., Haflidason, H., Hajdas, I., Hatté, C., Heaton, T.J., Hoffmann, D.L., Hogg, A.G., Hughen, K.A., Kaiser, K.F., Kromer, B., Manning, S.W., Niu, M., Reimer, R.W., Richards, D.A., Scott, E.M., Southon, J.R., Staff, R.A., Turney, C.S.M., van der Plicht, J., 2013. INTCAL13 and marine INTCAL13 radiocarbon age calibration curves 0–50,000 years cal BP. *Radiocarbon* 55, 1869–1887.
- Rittershofer, K.-F., 1987. Grabraub in der Bronzezeit. *Bericht der Römisch-Germanischen Kommission* 68, 5–23.
- Sandgathe, D.M., Dibble, H., Goldberg, P., McPherron, S.P., 2011. The Roc de Marsal Neanderthal child: a reassessment of its status as a deliberate burial. *Journal of Human Evolution* 61, 242–253.
- Shahack-Gross, R., Albert, R.M., Gilboa, A., Nagar-Hillman, O., Sharon, I., Weiner, S., 2005. Geoarchaeology In an Urban Context: the uses of space in a Phoenician monumental building at Tel Dor (Israel). *Journal of Archaeological Science* 32, 1417–1431.
- Shillito, L.-M., Ryan, P., 2013. Surfaces and streets: phytoliths, micromorphology and changing use of space at Neolithic Çatalhöyük (Turkey). *Antiquity* 87, 684–700.
- Shillito, L.-M., Bull, I.D., Matthews, W., Almond, M.J., Williams, J.M., Evershed, R.P., 2011. Biomolecular and micromorphological analysis of suspected faecal deposits at Neolithic Çatalhöyük, Turkey. *Journal of Archaeological Science* 38 (8), 1869–1877.
- Sprenger, S., 1999. *Zur Bedeutung des Grabraubes für sozioarchäologische Gräberfeldanalysen*. Eine Untersuchung am frühbronzezeitlichen Gräberfeld Franzhausen I. Niederösterreich, Berger, Wien.
- Stoops, G., 2003. *Guidelines for Analysis and Description of Soil Thin Sections*. Soil Science Society of America, Madison.
- Usai, M.R., Pickering, M.D., Wilson, C.A., Keely, B.J., Brothwell, D.R., 2014. ‘Interred with their bones’: soil micromorphology and chemistry in the study of human remains. *Antiquity* 88, Issue 339, Project Gallery, <http://antiquity.ac.uk/projgall/usai339/> (accessed 14.03.16).
- Van Haperen, M.C., 2010. Rest in pieces: an interpretive model of early medieval ‘grave robbery’. *Medieval and Modern Matters* 1, 1–36.
- Van Haperen, M.C., 2013. The distributed dead: personhood from the perspective of reopened graves. In: Ludowici, B. (Ed.), *Individual or Individuality? Approaches Towards an Archaeology of Personhood in the First Millennium AD*, pp. 89–94.
- Van Vliet-Lanoë, B., 2010. Frost action. In: Stoops, G., Marcelino, V., Mees, F. (Eds.), *Interpretation of Micromorphological Features of Soils and Regoliths*. Elsevier, Amsterdam, pp. 81–108.
- Weiner, S., 2010. *Microarchaeology: Beyond the Visible Archaeological Record*. University Press, Cambridge.
- Weninger, B., Clare, I., Jöris, O., Jung, R., Edinborough, K., 2015. Quantum theory of radiocarbon calibration. *World Archaeology* 47, 543–566.
- Zintl, S., 2012. Frühmittelalterliche Grabräuber? Wiedergeöffnete Gräber der Merowingerzeit im Raum Regensburg. In: Chytráček, M., Gruber, H., Michálek, J., Sandner, R., Schmotz, K. (Eds.), *Fines Transire*. 21. Treffen der Archäologischen Arbeitsgemeinschaft Ostbayern/West- und Südböhmen/Oberösterreich, 22.6. – 25.6. 2011 Stříbro, pp. 189–197.